Journal of Nuclear Materials 408 (2011) 102–109

Contents lists available at ScienceDirect

Journal of Nuclear Materials

journal homepage: www.elsevier.com/locate/jnucmat

Long-term product consistency test of simulated 90-19/Nd HLW glass

X.Y. Gan [a,*], Z.T. Zhang [a], W.Y. Yuan [b], L. Wang [a], Y. Bai [a], H. Ma [a]

[a] Radiochemistry Department, China Institute of Atomic Energy, P.O. Box 275(93), 102413 Beijing, People's Republic of China
[b] Environment Science & Engineering, Tsinghua University, 100084 Beijing, People's Republic of China

ARTICLE INFO

Article history:
Received 20 April 2010
Accepted 11 November 2010

ABSTRACT

Chemical durability of 90-19/Nd glass, a simulated high-level waste (HLW) glass in contact with the groundwater was investigated with a long-term product consistency test (PCT). Generally, it is difficult to observe the long term property of HLW glass due to the slow corrosion rate in a mild condition. In order to overcome this problem, increased contacting surface (S/V = 6000 m^{-1}) and elevated temperature (150 °C) were employed to accelerate the glass corrosion evolution. The micro-morphological characteristics of the glass surface and the secondary minerals formed after the glass alteration were analyzed by SEM-EDS and XRD, and concentrations of elements in the leaching solution were determined by ICP-AES. In our experiments, two types of minerals, which have great impact on glass dissolution, were found to form on 90-19/Nd HLW glass surface when it was subjected to a long-term leaching in the groundwater. One is Mg–Fe-rich phyllosilicates with honeycomb structure; the other is aluminosilicates (zeolites). Mg and Fe in the leaching solution participated in the formation of phyllosilicates. The main components of phyllosilicates in alteration products of 90-19/Nd HLW glass are nontronite ($Na_{0.3}Fe_2Si_4O_{10}(OH)_2{\cdot}4H_2O$) and montmorillonite ($Ca_{0.2}(Al,Mg)_2Si_4O_{10}(OH)_2{\cdot}4H_2O$), and those of aluminosilicates are mordenite ($(Na_2,K_2,Ca)Al_2Si_{10}O_{24}{\cdot}7H_2O$)) and clinoptilolite ($(Na,K,Ca)_5Al_6Si_{30}O_{72}{\cdot}18H_2O$). Minerals like $Ca(Mg)SO_4$ and $CaCO_3$ with low solubility limits are prone to form precipitant on the glass surface. Appearance of the phyllosilicates and aluminosilicates result in the dissolution rate of 90-19/Nd HLW glass resumed, which is increased by several times over the stable rate. As further dissolution of the glass, both B and Na in the glass were found to leach out in borax form.

1. Introduction

Chemical durability of high-level waste (HLW) glasses in contact with water is very important for performance assessment of the glass and validation of performance assessment models. The difficulty in studying of this property is in short laboratory timescale within which the glass evolution is hardly observed. Some methods such as natural [1] and archaeological analogs [2], predictive modeling [3] and acceleration corrosion tests [4] were developed and employed to solve this problem, and some successes about this aspect study have been also achieved in recent years [5,6].

90-19/Nd(U) glass (Nd or U as the surrogate of actinide nuclides), borosilicate glass form was developed to immobilize HLW in China in the early 1990s, and an underground repository site in Northwest of China is in the investigation and evaluation phase now. Meanwhile, the studies on the glass alteration under the disposal circumstance have been carried out by Chinese researchers as well. WU [7] studied the leaching behavior of 90-19/U HWL glass in deioned water at 90 °C, and discovered the pit corrosion and sediment appeared on the glass surface of a 6-day leaching test and no crystals separated from the glass forms. Shen [8,9] investigated the glass surface and element leaching characteristics of 90-19/U vitrified forms in pure water and the simulated underground water for 180 days, and concluded that temperature has a significant impact on the glass dissolution, and the alteration layer is depleted in Li, Na and B, and enriched in U, Fe, Ti, Mg and Ca with a different degree. Zhang [10] predicted the main element concentrations with PHREEQC code for a 546-day alteration test of 90-19/Nd HLW glass, and found minerals of Al_2O_3 and $CaCO_3$ on the glass surface at 150 °C corrosion. However, the previous studies only focused on the coupon static leaching test (MCC-1) with a small ratio of the surface area of the glass to the volume of the leaching solution (S/V), 10 m^{-1}. The method within a short period is difficult to reveal the chemical durability of HLW glass undergone the long-term alteration in the groundwater. Therefore, in this study a long-term product consistency test (PCT) at a large S/V (6000 m^{-1}) and a high temperature (150 °C) were adopted to speed the progress of the glass alteration. We found that PCT is an effective tool to rapidly screen and evaluate the chemical durability using elevated temperatures and large contacting surface. By

* Corresponding author. Tel.: +86 10 69358048; fax: +86 10 69358564.
E-mail address: xygan@126.com (X.Y. Gan).

0022-3115/$ - see front matter © 2010 Elsevier B.V. All rights reserved.
doi:10.1016/j.jnucmat.2010.11.020

a long time (730 days) of observation, we found that the chemical durability of 90-19/Nd HLW glass can be illustrated when it contacts with the groundwater under mild conditions.

2. Experimental

2.1. Materials and immersion vessel

A simulated HLW 90-19/Nd glass from cold tests of Chinese vitrification process was used in this study. This glass was remelted at 950 °C for 3 h and air quenched on a stainless steel plate to assure good homogenization. The water for PCT was collected from underground disposal site in China North-west and ultra-filtered by 10,000 MW-cutoff membrane filters. The compositions of glass in wt.% of oxides and water in mg/L of major ions are given in Tables 1 and 2, respectively. The vessel for immersing the glass in groundwater is a kind of hydrothermal reaction vessel which is composed of Teflon inner vessel and stainless steel outer vessel as shown in Fig. 1.

2.2. Procedure

The chemical durability of the glass was evaluated with a long-term PCT according to Test Method B of ASTM standard-C 1285-02(PCT-B) [11]. The glass was crushed and sieved, and the particles of 80–120 mesh (120–180 μm) collected, washed with ethanol in an ultrasonic bath, and then dried at room temperature. Approximately 15.00 ± 0.01 g of glass particles were added into each hydrothermal reaction vessel. The vessels were then transferred into a low oxygen glove box ($[O_2] < 10$ vppm), where about 40.0 ± 0.1 g water was added to each vessel before being sealed. The sealed vessels were placed into two ovens for PCT, respectively, at 90 ± 1.0 °C and 150 ± 1.0 °C for 7, 14, 28, 90, 180, 546 and 730 days. After each leaching period, three vessels were removed from each oven and cooled at room temperature, and then replaced in the low-oxygen box for solid–liquid separation with decantation, and pH value and oxidation–reduction potential measurement. The leaching solution was filtrated with a 0.45 μm membrane and acidified with a drop of concentrated HNO_3, and then stored in a closed plastic bottle for the element analysis. The glass particles was cleaned with ethanol three times and dried for surface analyses.

The specified surface area of the glass particles was about 0.035 m^2/g which was determined by the stereological analysis based on SEM observation, and S/V used was about 6000 m^{-1}. The underground water was placed into the low-oxygen box before-hand and kept for several days to ensure its oxidation–reduction potential falling in a range of −100–(−60) mv when used.

Table 1
Compositions of simulated 90-19/Nd HLW glass.

Oxide	Content (wt.%)	Oxide	Content (wt.%)	Oxide	Content (wt.%)
SiO_2	50.23	SrO	0.037	Fe_2O_3	3.14
B_2O_3	18.48	Y_2O_3	0.016	NiO	0.57
Na_2O	11.01	MoO_3	0.19	K_2O	0.090
Li_2O	1.93	MnO_2	0.016	P_2O_5	0.069
Al_2O_3	2.94	Cs_2O	0.11	SO_3	0.64
CaO	4.54	BaO	0.021	TiO_2	0.84
MgO	0.84	Nd_2O_3	1.97	Cr_2O_3	0.30

Table 2
Compositions of the underground water.

Element	Na^+	K^+	Ca^{2+}	Mg^{2+}	Fe (total)	F^-
Content (mg/L)	1027	16.1	206	51.2	0.25	1.89
Element	Cl^-	Br^-	CO_3^{2-}	NO_3^-	SO_4^{2-}	SiO_2 (total)
Content (mg/L)	1155	0.057	138	30.2	1074	13.1

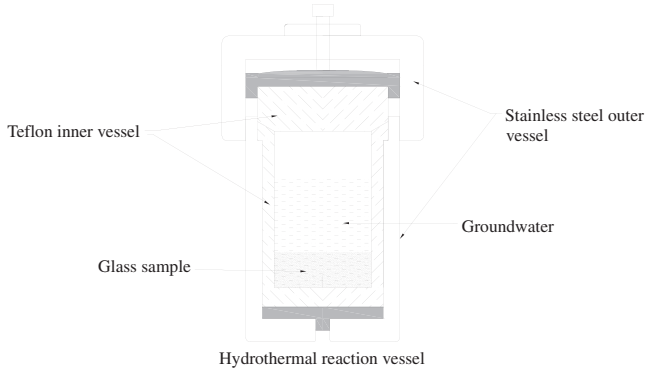

Fig. 1. Schematics of PCT immersion apparatus.

2.3. Analysis

An inductively coupled plasma atomic emission spectrometry (ICP-AES, VISTA-MPX, VERIN, USA) with a detective limit of 10^{-9} g/ml was used for the analysis of the concentrations of Li, Na, B, Si, Ca Mg and Nd in the leaching solution. The H^+ concentration and oxidation–reduction potential of the leaching solution were, respectively, determined with a glass pH combination electrode and a Pt-AgCl/Ag combination electrode on a pH-meter (HI9025, HANNA, ITALY). A field emission electron microscope (JSM-6301F, JEOL, JAPAN) equipped with a energy dispersive X-ray spectrometer (EDS, Oxford INCA300, OXFORD,UK) was employed to take microscopic images and element analysis of the sample surface at an accelerating voltage of 15 kV. Prior to performance of EDS analysis major elements in the glass, Na, Mg, Al, Si, Ca, Fe, Nd and S, were calibrated by corresponding standard substances, albite, MgO, Al_2O_3, SiO_2, Wollastonite, Fe, NdF_3 and FeS_2. Dot and rectangle sampling modes were taken for element analysis and the measured areas were 1 μm in diameter for a dot and more than 1um (wide) by 2 μm (long) for a rectangle. The analyzed sample was only treated with spraying C for conductivity. The secondary mineral phases of the alteration were identified and quantitated by a X-ray diffractometer (D_{max}-12 kW, Rigaku, JAPAN) at a scan rate of 8°(2θ)/min with Cu Kα radiation and the scanning mode of $\theta/2\theta$. When the analyzed sample contains n mineral phases, the weight percent of one mineral phase, x_i, is determined by the following formula:

$$x_i = \frac{I_i}{K_i} \Big/ \left\{ \sum_{j=1}^{n} \frac{I_j}{K_j} \right\} \tag{1}$$

where I_i is the diffraction strength of i mineral phase, K_i is a reference strength ratio of the maximum diffraction strength of i mineral to that of a given standard mineral at 1:1 weight mixture. The K_i values can be obtained from the power diffraction file (PDF) database compiled by International Centre for Diffraction Data (ICDD).

2.4. Calculation of alteration parameters

The glass alteration rates were determined by the normalized mass loss of element, which is defined in the following relation:

$$NL_i = \frac{C_i \cdot V}{SA \cdot f_i} \tag{2}$$

where NL_i is the normalized mass loss of element i ($g\,m^{-2}$), C_i is the concentration of element i in the solution ($g\,L^{-1}$), V is the volume of

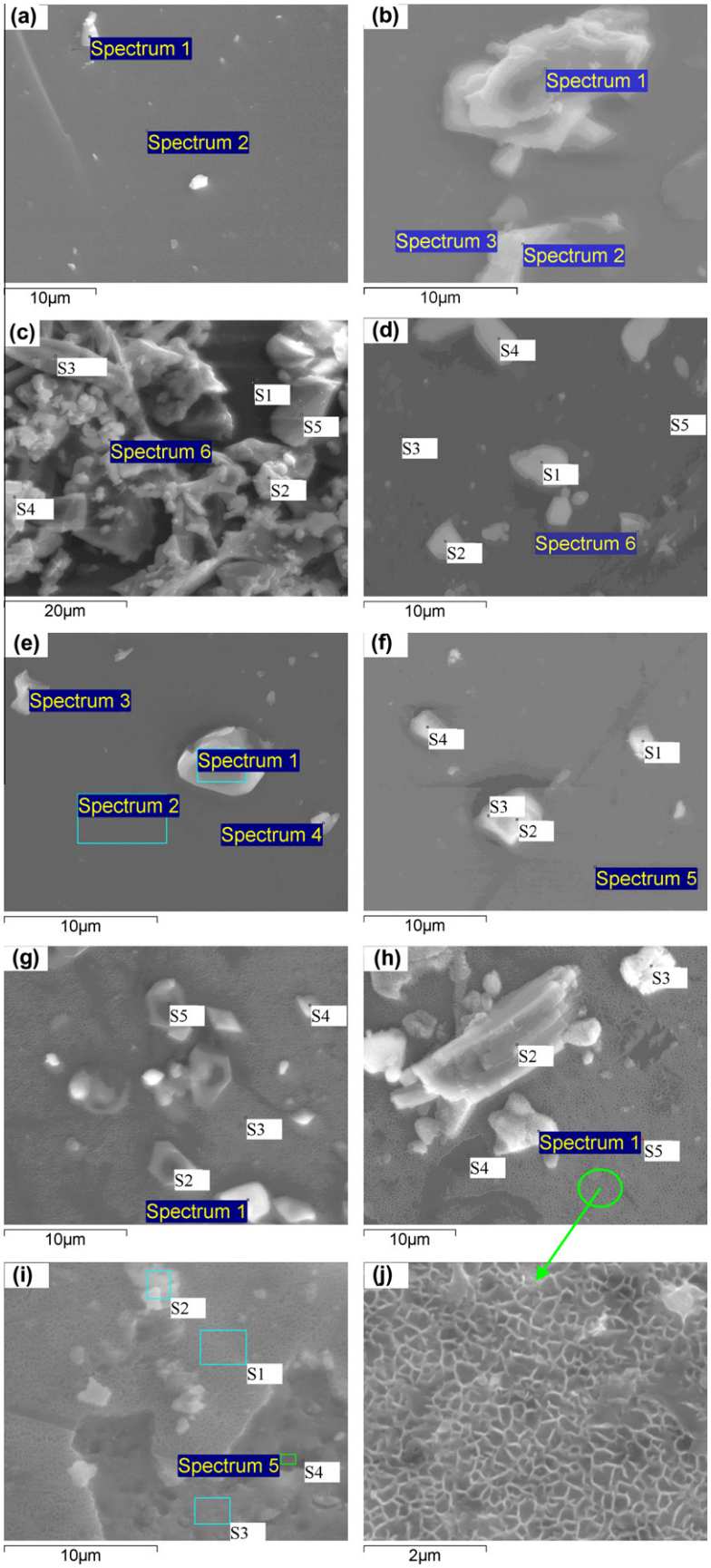

Fig. 2. The secondary electron photograph of simulated 90-19/Nd HLW glass surface ((a) original glass surface; (b–e) glass surface leaching at 90 °C for 7, 14, 28 and 730 days; (f–i) glass surface leaching at 150 °C for 28, 90, 180 and 730 days; (j) magnification of partial region of sample h).

the leaching solution (L), SA is the surface area of the glass (m^2), f_i is the mass fraction of element i in the glass. As the variation of the normalized mass loss of element i with time t follows an exponential function, that is, $NL_i = a\ exp(t/b) + c$, the glass alteration rate at each time is calculated by:

$$r_i = \frac{\partial NL_{(i)}}{\partial t} = \frac{a}{b}\exp(t/b) \tag{3}$$

When the evolution of the normalized mass loss is irregular or difficult to be fitted with one regression function, the alteration rate between two sampling points is calculated by the relation:

$$r(i)_{\frac{t+(t+1)}{2}} = \frac{NL(i)_{t+1} - NL(i)t}{(t+1) - t} \tag{4}$$

3. Results and Discuss

3.1. SEM-EDS

Fig. 2 shows SEM images of glass surfaces after PCT for different test durations and two temperatures. Table 3 shows the results of EDS analysis for glass surfaces as a function of PCT time and temperature. The glass tested for 730 days at 90 °C (Fig. 2e) did not show any signs of corrosion and its elemental composition was about the same as for the original glass (Fig. 2a). In contrast, a layer of honeycomb structure formed on the glass surfaces after 90 days at 150 °C (Fig. 2g) and became more pronounced at longer times. This structure was observed under several experimental cases for different glasses. It formed on basaltic glass [12] in $MgCl_2$–$CaCl_2$ solution for 24 days at 190 °C, on R7T7 reference glass [13] in pure water at 150 °C with $S/V = 8000\ m^{-1}$ after 111 days and on SON68 glass [14] in NaOH solution after 14 days. The elemental compositions of the glass surface also changed with 150 °C. Mg, Fe and Nd were richen, and Na and Al were depleted with the time. As the honeycomb layer grew thick, it began to peel off, and pitting corrosions appeared in the below surface of the 730-day glass (Fig. 2i). Table 4 shows the results of EDS analysis for different sampled areas in Fig. 2i. In comparison with the original glass (Table 3), we found that the below surface contained Mg and Fe more than the original glass and the pitting area, and less than the peeling piece and the honeycomb layer. It was suggested that Mg and Fe came from the leaching solution and participated in the formation of the surface layer.

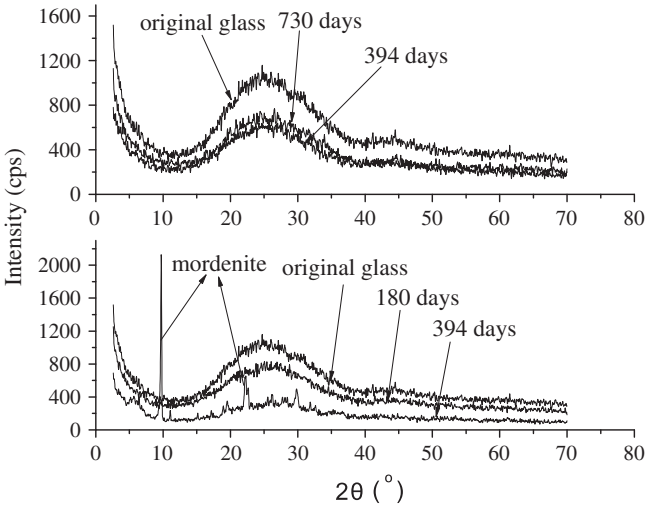

Fig. 3. X-ray diffraction spectrum of simulated 90-19/Nd HLW glass (The upper is for 90 °C alteration, the below for 150 °C alteration).

Moreover, some of crystals with particle or batt shapes developed on the glass surface of different durations at two temperatures. Table 5 shows elemental compositions of the crystals, which appeared in the SEM images in Fig. 2 and marked with "S" or "Spectrum". The crystalline phases with high S and Ca contents formed at 90 °C for 7 and 28 days were considered to be $Ca(Mg)SO_4$ (Fig. 2b Spectrum1, Spectrum 2 and Fig. 2d Spectrum 6) because the atom ratio of (Ca + Mg) to S in them is close to 1, and also because the immersion solution is high brine groundwater and

Table 3
Element content of simulated 90-19/Nd HLW glass surface.

T (°C)	Duration (day)	Element content (at.%)								
		Na	Mg	Al	Si	Ca	Ti	Fe	Nd	O
90	0	7.56 ± 0.44	0.22 ± 0.24	2.10 ± 0.36	23.02 ± 2.60	3.62 ± 1.51	0.38 ± 0.21	1.41 ± 0.17	0.16 ± 0.18	61.54 ± 1.74
	7	8.15 ± 0.65	0.56 ± 0.07	2.85 ± 0.88	23.92 ± 0.60	2.00 ± 0.18	0.31 ± 0.01	1.09 ± 0.14	0.17 ± 0.15	60.94 ± 0.42
	394	6.18 ± 2.83	0.47 ± 0.09	2.45 ± 0.72	23.68 ± 1.60	2.66 ± 0.59	0.41 ± 0.18	2.18 ± 1.82	0.53 ± 0.30	61.43 ± 1.73
	730	6.15 ± 2.06	0.72 ± 0.52	2.36 ± 0.24	24.24 ± 0.63	2.69 ± 0.48	0.34 ± 0.02	1.36 ± 0.07	0.29 ± 0.01	61.85 ± 0.43
150	0	7.56 ± 0.44	**0.22 ± 0.24**	2.10 ± 0.36	23.02 ± 2.60	3.62 ± 1.51	0.38 ± 0.21	**1.41 ± 0.17**	**0.16 ± 0.18**	61.54 ± 1.74
	7	6.05 ± 1.33	**0.56 ± 0.08**	2.30 ± 0.04	24.42 ± 0.17	2.38 ± 0.29	0.35 ± 0.06	**1.33 ± 0.16**	**0.34 ± 0.06**	62.26 ± 0.50
	394	3.10 ± 0.60	**1.46 ± 0.35**	1.04 ± 0.39	23.58 ± 0.31	2.17 ± 0.34	0.62 ± 0.14	**5.27 ± 0.50**	**0.35 ± 0.02**	62.40 ± 0.17
	730	5.06 ± 0.75	**1.26 ± 0.36**	0.77 ± 0.02	22.47 ± 0.25	2.49 ± 0.85	0.59 ± 0.09	**5.81 ± 1.22**	**0.41 ± 0.10**	61.14 ± 0.23

T: temperature.

Table 4
Elemental compositions of sampled areas on the glass of 730 days at 150 °C (see Fig. 2i).

Element	Honeycomb layer (S1)	Peeling piece (S2)	Below surface (S3)	Pitting area (S4)	Pitting area (Spectrum 5)
Na K	4.72	4.45	4.87	3.83	3.65
Mg K	**1.38**	**2.77**	**1.06**	**0.83**	**0.99**
Al K	0.79	1.22	0.79	0.79	0.67
Si K	22.31	21.46	22.44	23.96	23.46
S K	0.00	0.00	0.00	0.00	0.00
Cl K	0.14	0.00	0.16	0.12	0.00
Ca K	2.35	1.19	3.03	4.10	3.78
Fe K	**6.51**	**7.37**	**5.67**	**3.38**	**4.35**
Nd L	0.38	0.16	0.49	0.55	0.49
O	61.41	61.37	61.48	62.43	62.61

Table 5
Elemental compositions of crystals and the near glass in SEM images of Fig. 2 (Atom%).

Element	Fig. 2b (7 days, 90 °C)			Fig. 2c (14 days, 90 °C)					
	Spectrum1	Spectrum2	Spectrum3	S1	S2	S3	S4	S5	Spectrum6
Na K	1.79	2.86	8.44	4.80	4.03	5.91	2.91	9.08	4.20
Mg K	0.84	0.00	0.49	2.31	**5.54**	**4.25**	**6.66**	1.50	**8.29**
Al K	0.43	0.62	2.35	2.35	2.42	2.13	1.92	2.05	2.04
Si K	5.78	5.60	24.15	22.28	22.66	23.26	22.46	22.36	21.49
S K	**13.31**	**12.87**	0.00	1.24	0.33	0.00	0.24	0.42	0.48
Cl K	0.00	0.00	0.00	1.12	1.13	0.34	1.10	1.61	1.08
Ca K	**11.99**	**12.93**	2.14	2.92	2.21	2.01	2.04	2.04	1.53
Fe K	0.00	0.00	1.24	1.09	1.00	0.98	1.25	0.97	0.68
Nd L	0.00	0.00	0.26	0.28	0.00	0.24	0.24	0.27	0.00
O	65.86	65.12	60.93	61.60	60.68	60.88	61.18	59.55	60.20
	Fig. 2d (28 days, 90 °C)						Fig. 2e (730 days, 90 °C)			
	S1	S2	S3	S4	S5	Spectrum6	Spectrum1	Spectrum2	Spectrum3	Spectrum4
Na K	**18.84**	**35.65**	3.60	**35.36**	2.98	5.82	1.95	6.96	6.65	6.55
Mg K	0.79	0.00	0.47	0.00	0.48	0.43	1.14	0.39	0.55	0.68
Al K	1.72	0.50	2.82	0.60	2.75	2.05	0.66	2.32	2.36	2.43
Si K	16.30	3.93	24.93	4.75	25.14	17.85	5.25	24.12	24.33	24.36
S K	0.00	0.22	0.35	0.00	0.24	**4.77**	1.23	0.00	0.24	0.00
Cl K	**10.30**	**31.64**	0.49	**30.38**	0.64	0.48	0.39	0.00	0.00	0.23
Ca K	1.58	0.48	2.78	0.41	3.03	**4.54**	**36.05**	2.57	2.63	2.55
Fe K	0.97	0.00	1.43	0.00	1.42	0.93	0.00	1.40	1.06	1.08
Nd L	0.18	0.00	0.27	0.00	0.32	0.22	0.00	0.29	0.00	0.29
O	49.32	27.57	62.86	28.50	62.98	62.90	**53.33**	61.94	62.17	61.84
	Fig. 2f (28 days, 150 °C)					Fig. 2g (90 days, 150 °C)				
	S1	S2	S3	S4	Spectrum5	Spectrum1	S2	S3	S4	S5
Na K	8.59	8.48	8.08	7.86	6.95	4.36	**9.85**	1.97	**3.05**	**10.96**
Mg K	0.59	0.64	0.49	0.68	0.45	1.05	1.15	1.14	1.75	1.06
Al K	2.27	2.44	2.39	2.34	2.31	**5.37**	2.18	2.00	2.75	2.04
Si K	23.56	23.87	23.58	24.03	24.28	**24.36**	20.01	17.19	24.15	18.62
S K	0.30	0.00	0.24	0.00	0.24	0.33	2.07	0.23	0.38	2.87
Cl K	0.13	0.00	0.00	0.00	0.00	0.16	0.26	0.13	0.33	0.23
Ca K	2.20	2.07	2.21	2.34	2.21	0.74	2.33	0.00	2.73	2.15
Fe K	1.13	1.07	1.28	1.08	1.24	0.50	1.23	1.15	1.54	1.43
Nd L	0.27	0.28	0.31	0.27	0.30	0.12	0.38	0.31	0.36	0.33
O	60.95	61.14	61.42	61.39	62.01	63.00	60.54	75.87	62.95	60.32
	Fig. 2h (180 days, 150 °C)									
	Spectrum1	S2	S3	S4	S5					
Na K	4.47	3.25	4.05	4.78	2.21					
Mg K	1.17	0.00	4.16	0.41	0.56					
Al K	2.16	**6.09**	3.40	2.04	2.19					
Si K	24.75	**26.53**	23.46	25.44	25.42					
S K	0.00	0.00	0.24	0.23	0.38					
Cl K	0.20	0.00	1.46	0.00	0.17					
Ca K	2.30	0.00	0.87	2.73	3.38					
Fe K	1.69	0.00	1.08	1.31	1.75					
Nd L	0.38	0.00	0.00	0.32	0.41					
O	62.87	64.13	61.28	62.74	63.52					

contains a considerable amount of Cl^-, Na^+, CO_3^{2-}, SO_4^{2-} etc. ions. For the latter reason, Na–Cl-rich crystals formed at 90 °C for 28 days (Fig. 2d-S1, S2 and S4) and a Ca-rich crystal for 730 days (Fig. 2e spectrum1) were considered to be $CaCO_3$ and NaCl. There were some other crystalline phases that were difficult to be identified such as Mg-rich crystals on the glass tested for 14 days at 90 °C (Fig. 2c S2,S3,S4 and S6) and the crystals with a large Al–Si ratio for 90 and 180 days at 150 °C (Fig. 2g Spectrum 1 and Fig. 2h S2). Besides, some looked like crystals were tiny glass particles probably for their composition similar to the near glass (Fig. 2e Spectrums 3 and 4).

3.2. XRD

XRD analysis was employed in this study to identify and semi-quantify the secondary crystalline phases that formed during the glass alteration. Fig. 3 shows XRD patterns for the original amorphous glass and the glasses after leaching test at 90 °C for 394 and 730 days and at 150 °C for 180 and 394 days. No crystalline phases were detected by XRD in the glass samples after leaching at 90 °C. On the other hand, different crystalline phases were identified in the glasses after leaching at 150 °C for 394 and more days. These phases are quantified in the Table 6. The noncrystalline proportion in the glasses decreased from 73% (wt.%) at the 394th day to 37% at 730th day. The major crystals were mordenite ($(Na_2,K_2,Ca)Al_2Si_{10}O_{24}\cdot 7H_2O$), clinoptilolite ($(Na,K,Ca)_5Al_6Si_{30}O_{72}\cdot 18H_2O$) and nontronite ($Na_{0.3}Fe_2Si_4O_{10}(OH)_2\cdot 4H_2O$), and the minor were montmorillonite ($Ca_{0.2}(Al,Mg)_2Si_4O_{10}(OH)_2\cdot 4H_2O$), kaolinite ($Al_2Si_2O_5(OH)_4$) and zeolite ($Na_{3.6}Al_{3.6}Si_{12.4}O_{32}\cdot 14H_2O$).

These crystalline phases belong to two groups of minerals. One group is phyllosilicates and the other is aluminosilicates. Phyllosilicates take on honeycomb morphological characteristics and the elements of Mg, Fe, Ni etc. are prone to be seated in them. Therefore, the Mg–Fe-rich honeycomb structure formed on 90-19/Nd glass surface

Table 6
The mineral phase content in 90-19/Nd HLW glass at 150 °C.

No.	Duration (day)	Crystalline phase proportion (wt.%)						Noncrystalline proportion (%)
		Mordenite (%)	Montmorillonite (%)	Kaolinite (%)	Clinoptilolite (%)	Nontronite (%)	Zeolite (%)	
1	394	12	2	–	13	–		73
2	546	23			16	5	4	53
3	730	33	–	4	13	13		37

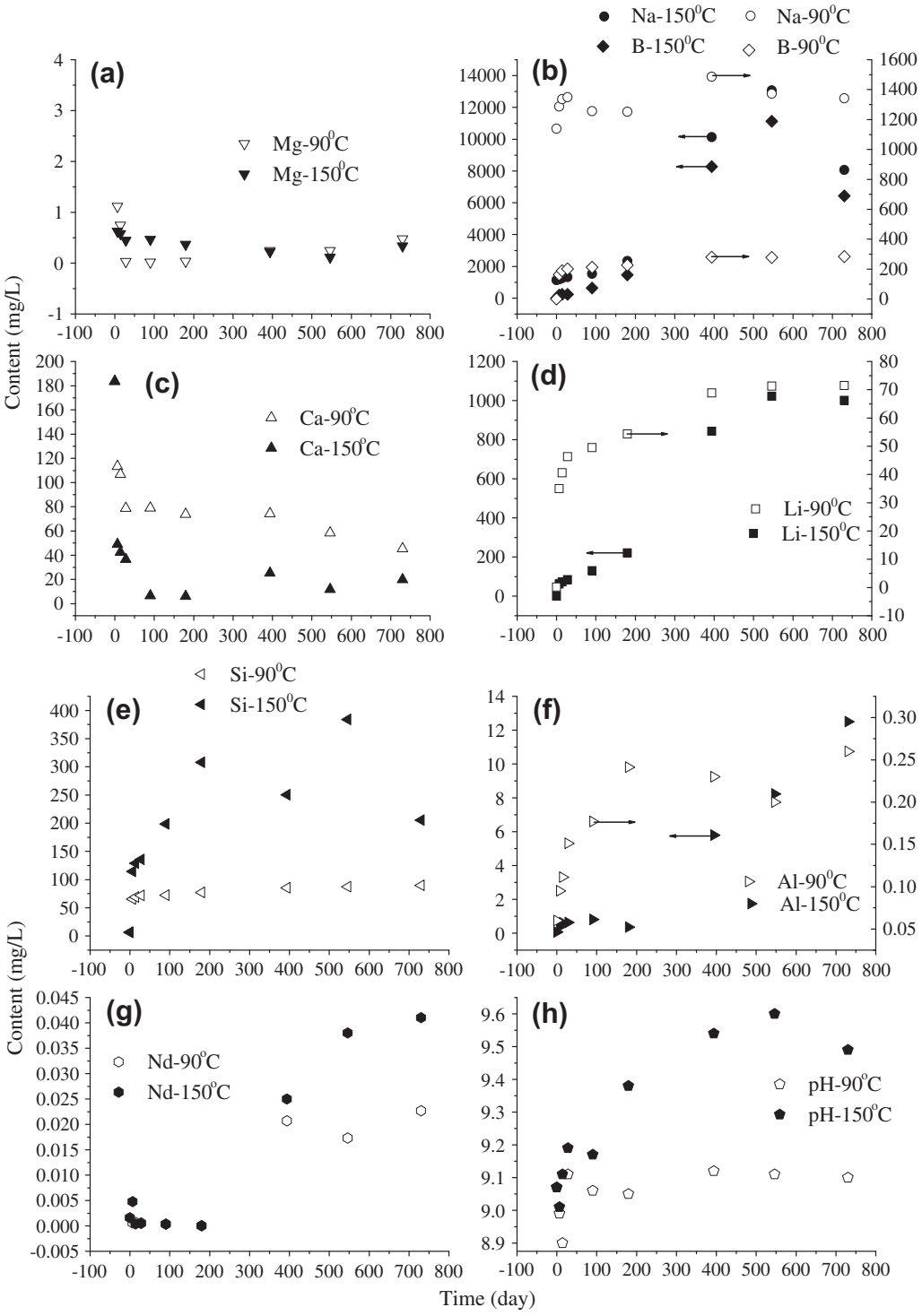

Fig. 4. Evolution of main element concentrations in the leaching solution with time (Static leaching, $S/V = 6000\ m^{-1}$, $[O_2] < 10$vppm, leaching solution: the underground water).

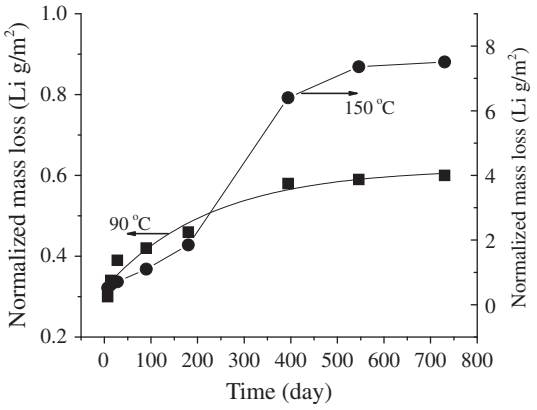

Fig. 5. Evolution of the normalized mass losses of Li with time (Static leaching, $S/V = 6000\ m^{-1}$, $[O_2] < 10$vppm, leaching solution: the underground water).

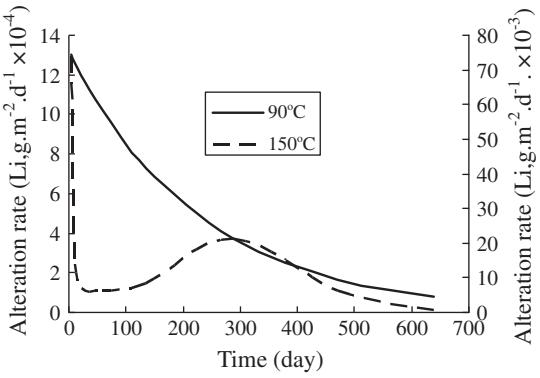

Fig. 6. Alteration rate (Li, g m^{-2} d^{-1}) of 90-19/Nd HLW glass at 90 °C and 150 °C.

Table 7
Leaching rate of main glass elements in atmosphere and low oxygen conditions [20]. (Experimental conditions: $S/V = 10\ m^{-1}$, 90 °C, de-ion water.)

Element	Leaching rate (g m^{-2} d^{-1})	
	Atmosphere condition	Low oxygen condition
Si	0.664	0.366
Na	0.854	0.502
B	0.926	0.484
Sr	0.184	0.150
Cs	0.734	0.403
Nd	4.1×10^{-5}	1.1×10^{-5}

was phyllosilicates, and its main components were nontronite and montmorillonite. Different minerals of phyllosilicates were found in glass alteration products. Mg–Al-rich semctite and nontronite($(Na,K)_{0.8}(Fe,Mg)_{1.3}(Al,Si)_4O_{10}$) were determined on the basaltic glass [12] and the glass formulated to immobilize West Valley nuclear waste [15]. Sauconite ($Na_{0.3}Zn_3Si_3AlO_{10}(OH)_2{\cdot}4(H_2O)$), pimelite ($Ni_3Si_4O_{10}(OH)_2{\cdot}5(H_2O)$) and nontronite ($Na_{0.3}Fe^{3+}{}_2Si_3AlO_{10}(OH)_2{\cdot}4(H_2O)$) were detected in the alteration products from the SON68 glass [16].

Mordenite, clinoptilolite, kaolinnite and zeolite belong to aluminosilicates. Aluminosilicates like phyllosilicates also existed in several forms under different conditions for glass alteration test. For SON68 glass [5] zeolite phases were likely to precipitate at temperatures exceeding 150 °C or at pH values above 10 at 90 °C. Under hydrothermal conditions with presence of a volcanic glass [17], clinoptilolite formation was favored in a K-rich solution for more than one week at temperature less than 150 °C, and mordenite formation in a Na-rich solution at temperature greater than 140 °C. In 8-day runs at 140 °C, clinoptilolite formation was favored by liquid:solid reactant (volume:mass) ratios less than 1.0 and mordenite by the ratios from 0.85 to 1.5. The mechanism of formation of the different aluminosilicates may involve in silicacyclic tetramers which are abundant in concentrated solutions under alkaline hydrothermal conditions while almost absent in low-temperature dilute solutions.

3.3. ICP-AES

3.3.1. Elemental leaching

Fig. 4 shows the change in concentration of selected elements and pH of solution over the time for 90 and 150 °C. At 90 °C the concentrations of Li, Na, B, Si, Al and pH of the leaching solution increased with time while that of Ca and Mg decreased, and then stabilized after 28 days. Nd was leached out on the 180th day. The reason for the Ca and Mg decrease was in the formation of crystals like $CaCO_3$, $CaSO_4$, $MgSO_4$ etc.

At 150 °C, the Li, Na, B, Al and Nd concentrations and pH of the leaching solution increased between 180 and 546 days rapidly, and then Li and Nd became stable, Al was still increasing and Na, B and pH value were decreasing. The concentration increased rapidly is due to the secondary minerals—aluminosilicates and phyllosilicates mentioned above. Their formation triggered the further dissolution of the glass net structure. The decrease in the B and Na concentrations (Fig. 4b) is for the sampling and analysis that were carried out at the ambient temperature and resulted in some colorless precipitations separated out of the leaching solution. The precipitations were identified to be tincalconite ($Na_2B_4O_7{\cdot}5H_2O$) by XRD analysis. Furthermore, noticed that there was a close relevancy between the B and the Na concentration at 150 °C, and especially on the 394th, 546th and 730th day the mole ratios of Na to B in the leaching solution were very close to 1:2. Therefore, it was considered that the dissolution or precipitation of B and Na proceeded in the form of $Na_2B_4O_7$ within this period. However, the standpoint of the secondary mineral phases is difficult to clarify the increase in the Al concentration (Fig. 4f) because it contributed to the formation of both aluminosilicates and phyllosilicates and its concentration should decrease. As a matter of fact, the concentration is controlled by the solubility limit of aluminosilicates. Sin [18]studied the alteration of SON68 glass at 90 °C with a S/V ratio of 6500 m^{-1} and found that, below pH < 10, aluminosilicates were unlikely to precipitate and the gel layer of glass remained stable. In this study, pH of the leaching solution kept about 9.5 that led to part dissolution of aluminosilicates and sustained the concentration increase of Al. Since Si also participated in the formation of two minerals, it fluctuated between 200 mg/L and 375 mg/L after 180 days (Fig. 4e). The evolution of the Ca and Mg concentrations was similar to that at 90 °C for the same reason. The pH increase (Fig. 4h) is for the following reaction between the water molecular and the glass pristine.

$$(\equiv Si \cdot ONa) + H_2O \rightarrow (\equiv Si \cdot OH) + HO^- + Na^+$$

Zhang [10] and Shen [9] investigated the effects of the temperature, S/V, the atmosphere or the low oxygen condition and the underground water or the de-ion water on pH of the leaching solution of 90-19/Nd(U) glass. They summarized that pH of the solution in the high temperature, the low oxygen or the de-ion water is greater than that in the low temperature, the atmosphere or the underground water; and the larger S/V is, the higher pH under the other conditions in the same. Basically our studies got very similar results. In comparison between the two temperatures, whether the increases of pH and the Li, Na, B, Si and Al concentrations or the decreases of the Ca and Mg concentrations, the varying degrees were more at 150 °C than at 90 °C.

In addition, the oxidation–reduction potential of the leaching solution absented regularity for complicacy of the leaching system, but it was varying within (−300 to 0) mv for 150 °C test and (−60 to 0) mv for 90 °C test.

3.3.2. Alteration rate

The variations of the Li concentration with time exhibited good regularities at both temperatures (Fig. 4d), therefore, Li was used as an indicator to evaluate the dissolution rate of the glass. Fig. 5 shows the time dependent normalized mass loss of Li from the surface of glass samples at 90 °C and 150 °C. The experimental data of the former was fitted with exponential Eq. (5). The Eq. (6), the derivative of exponential fit, was used to calculate the glass dissolution rate. A suitable function was unavailable to fit the mass loss of Li at 150 °C, thus the Eq. (4) was employed to determine its rate.

$$NL_{Li} = -0.30\exp(t/-227) + 0.62 \ (R^2 = 0.97) \quad (5)$$

$$r_{Li} = \frac{\partial NL_{(Li)}}{\partial t} = 0.0011\exp(t/-227) \quad (6)$$

The glass alteration rate at 150 °C displayed a more complex evolution involving in the initial drop, stabilization, resumption and decrease within the experimental duration as shown in Fig. 6. The initial drastic decrease in the rate attributes to the rapid densification of gel layer probably, which usually forms on glass surface under contact with water and serves as a barrier to prevent the glass dissolving. The resumption of alteration rate is due to the mineral phases, which can degrade the gel layer and restart dissolution of the glass. In this study, the restarting time was on the 100th day or so, and just the time of the formation of Mg–Fe-rich phyllosilicates. That phyllosilicates can recover the glass dissolution was also supported by experiments conducted by Chave [16]. He added Zn^{2+} and Ni^{2+} to immersion solution of the glass, and that led to the formation of sauconite, hemimorphite (for Zn) and pimelite (for Ni), thereby sustained the glass dissolution near the initial rate. But the maximum resumption rate in this study was about 2×10^{-2} ($g\,m^{-2}\,d^{-1}$), and much less than the initial rate, 7×10^{-2} ($g\,m^{-2}\,d^{-1}$), but about four times as the stable rate. Furthermore, aluminosilicates (zeolites) are another important factor that renewed the glass dissolution, which consumed the aluminum and silicon in the gel [14]. Gauthier [19] verified that the alteration rate of R7T7 glass in contact with water containing zeolites was two times larger than those in pure water in the initial phase. The alteration rate at 90 °C decreased with time monotonously, and less than that at 150 °C by roughly an order of magnitude. The low oxygen condition can cause the leaching rate of main elements of 90-19/Nd glass to be slow, which was demonstrated by Zhang et al. [20] by an experimental comparison with the atmospheric condition (Table 7).

Kinetic study [5,6] shows that nuclear glass dissolution goes through 4 regimes: initial rate, rate drop, rate residue and rate resume under very particular circumstances, and corresponding alteration mechanisms are H^+/alkali inter-diffusion and silicate hydrolysis, gel layer formation or reaction affinity diminishing, water diffusion or phase precipitation. Judged from this, the alteration rate of 90-19/Nd glass at 150 °C had undergone the entire regimes while that at 90 °C was still settling in the first three regimes.

4. Conclusions

Chemical durability of simulated 90-19/Nd HWL glass in the groundwater was investigated with the long-term PCT method with $S/V = 6000\ m^{-1}$ at 150 °C and 90 °C. Some conclusions were obtained as follows.

The glass surface turned into honeycomb at the elevated temperature test after a certain immersion period. The honeycomb structure was a type of mineral named phyllosilicates which was comprised of nontronite ($Na_{0.3}Fe_2Si_4O_{10}(OH)_2{\cdot}4H_2O$) and montmorillonite ($(Ca_{0.2}(Al,Mg)_2Si_4O_{10}(OH)_2{\cdot}4H_2O$). Mg and Fe in the groundwater were prone to participate in the phyllosilicate formation. The Mg–Fe-rich phyllosilicates can resume the glass dissolution and accelerate the alteration rate of the glass. Another type of important mineral was aluminosilicates, which included mordenite ($(Na_2,K_2,Ca)Al_2Si_{10}O_{24}{\cdot}7H_2O$) and clinoptilolite ($(Na,K,Ca)_5Al_6Si_{30}O_{72}{\cdot}18H_2O$) etc. and formed at the elevated temperature as well. aluminosilicates also can renewed the glass dissolution. The maximum renewed rate was about four times as the stable rate. Some minor minerals like $Ca(Mg)SO_4$, $CaCO_3$ etc., which have low solubility limits, are like to form precipitant on the glass in the early alteration. Both B and Na in the glass leached out in borax form as the renewal of dissolution of the glass.

Minerals with poor crystallization or little amount are needed to be further identified by a suitable analysis method. The impact of mono-mineral on 90-19/Nd HWL glass dissolution remains to be further studied.

Acknowledgements

The authors would like to thank the Commission on Science, Technology, and Industry for National Defense (COSTIND) for financially supporting this research under Contract No. A0120060591, and also thank Dr. H.J. Jin of PNNL, USA for his help in the manuscript preparation.

References

[1] J.L. Crovisier, T. Advocat, J.L. Dussossoy, J. Nucl. Mater. 321 (2003) 91.
[2] S. Gin, J.L. Chouchan, D. Foy, Mater. Res. Soc. Symp. Proc. 932 (2006).
[3] P. Jollivet, Y. Minet, E. Vernaz, J. Nucl. Mater. 281 (2000) 231.
[4] W.L.Ebert, A.J.Bakel, in: Argonne National Laboratory(USA), ANL-CMT-CP-88456 Ed., 1996.
[5] P. Frugier, S. Gin, Y. Minet, T. Chave, B. Bonin, N. Godon, J.E. Lartigue, P. Jollivet, A. Ayral, L.D. Windt, G. Santarini, J. Nucl. Mater. 380 (2008) 8.
[6] E. Vernaz, S. Gin, C. Jegou, I. Ribet, J. Nucl. Mater. 298 (2001) 27.
[7] Z.G. Wu, S.G. Luo, C.Z. Yu, J.W. Shen, D.L. Liu, Chi. J. Nucl. Sci. Eng. 16 (1996) 87.
[8] J.W. Shen, S.G. Luo, B.L. Tang, D.L. Liu, Radiat. Prot. 16 (1996) 114.
[9] J.W. Shen, S.G. Luo, B.L. Tang, J. Nucl. Radiochem. 18 (1996) 79.
[10] H. Zhang, PhD thesis, China Institute of Atomic Energy, China, 2005.
[11] ASTM C1285-02, Standard test methods for determining chemical durability of nuclear, hazardous, and mixed waste glasses and multiphase glass ceramics: The product consistency test (PCT).
[12] A. Abdelouas, J.L. Crovisier, W. Lutze, B. Fritz, A. Mosser, R. Muller, Clay Clay Miner 42 (1994) 526.
[13] S. Gin, N. Godon, I. Ribet, P. Jollivet, Y. Minet, P. Frugier, E. Vernaz, J.M. Cavedon, B. Bonin, R.D. Quang, Mat. Res. Soc. Symp. Proc. 824 (2004).
[14] S. Ribet, S. Gin, J. Nucl. Mater. 324 (2004) 152.
[15] I.S. Muller, S. Ribet, I.L. Pegg, S. Gin, P. Frugier, American Ceramic Society, 176., Baltimore, USA, 2005. p. 191.
[16] T. Chave, in: Université Montpellier II – Science et Technique du Languedoc, 2008, p. 1.
[17] D.B. Hawkins, Clay Clay Miner 29 (1981) 331.
[18] S. Gin, J.P. Mestre, J. Nucl. Mater. 295 (2001) 83.
[19] A. Gauthier, J.H. Thomassin, P.L. Coustumer, Sciences de la terre et des planètes 329 (1999) 331.
[20] H. Zhang, S.G. Luo, Y.Z. Jiang, H. Zhou, J. Nucl. Radiochem. 27 (2005) 144.